

Development of a hermetically sealed Stirling engine battery charger

D M Clucas, BE, PhD and J K Raine, BE, PhD, CEng, FIMechE, FIPENZ, MSAE-A
Department of Mechanical Engineering, University of Canterbury, Christchurch, New Zealand

Recent Stirling engine research at the University of Canterbury has focused on the development of a compact 12 volt 200 watt electrical battery charger suitable for use in yachts, mobile homes or remote dwellings, and intended for scaling up to larger power applications. The hermetically sealed engine with integral alternator uses a four-cylinder double-acting configuration with air pressurized to 1 MPa as the working fluid. The engine and battery charger control system includes self-regulation, and automatic start and shut-down. The previous paper has described the wobble yoke mechanism which is central to the engine design as it requires only pre-lubricated single degree of freedom bearings. This paper explains the design philosophy behind the new engine and describes the computer modelling and subsequent development of engine components on an alpha configuration experimental prototype. Features examined include the alternator, the cylinder-mounted seals and the heat exchangers. Embodiment design features of the final double-acting prototype are discussed. Performance data for the experimental prototype are presented.

NOTATION

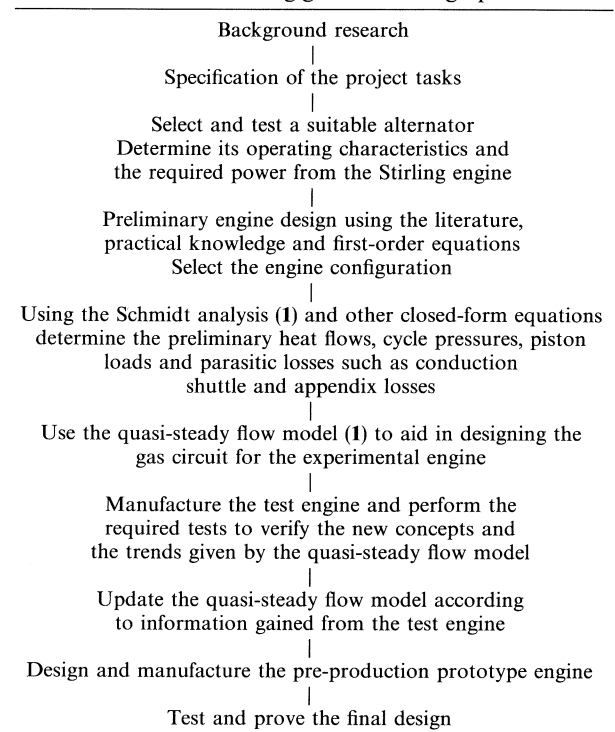
BP	brake power (W)
f	engine cyclic frequency (Hz)
HX	abbreviation for heat exchanger
P	cycle pressure (Pa)
P_{mean}	mean cycle pressure (Pa)
T_{H}	heater temperature (K)
T_{K}	cooler temperature (K)
V	cycle instantaneous volume (m^3)
V_0	total cycle volume variation (m^3)
W_n	empirical West number for scaling power output
η_{th}	ideal cycle thermal efficiency

1 INTRODUCTION

The Stirling engine has much to offer in power generation applications which require a quiet and clean alternative to the internal combustion engine. Development of Stirling cycle machines at the University of Canterbury began with the aim of producing a battery charger unit for yachts. Powering of auxiliary devices by the main diesel propulsion engine is noisy and often inefficient, with the diesel running at very light load and/or the batteries being charged at rates that are detrimental to battery life.

Another potentially important application appears to be in dwellings where it is uneconomic to connect to the mains power supply or where this supply is unreliable. It was determined that the yacht battery charger application could be as low as 200 W electrical output for a 12 V d.c. battery bank and the domestic dwelling requirement could be up to 3 kW a.c. electrical power at 230 V for a modern home. Both applications have particular value as a combined heat and power system since much of the rejected heat from the Stirling engine can be used to furnish the hot water supply and space heating for the dwelling. The prototype development concentrated on the 200 W d.c. system, designed on the

Table 1 The Stirling generator design process



basis that the engine form would be scaled up to outputs suitable for domestic power generation systems.

Table 1 shows the systematic but necessary iterative approach to design used in this project to produce a prototype for a commercial Stirling engine system. The previous paper (2) has described the theory and physical layout of the wobble yoke mechanism which was central to the engine design. The present paper describes the engine design, computer simulation work and performance of an alpha configuration experimental engine. Brief performance figures are given for the double-acting prototype intended for commercial development.

The MS was received on 29 December 1993 and was accepted for publication on 22 August 1994.

2 CONCEPTUAL BACKGROUND TO THE DESIGN

The direct competitors for a 200 W electrical output Stirling engine generator unit for battery charging use small internal combustion engines, wind power, photovoltaic cells and, in the case of yachts, tow generators which require the vessel to move (3). All of these have disadvantages relating to noise, weather or plant location. Bartolini *et al.* (4) and Walker *et al.* (5) report other recent Stirling engine developments of this kind. The 200 W electrical power output was determined through a study of daily electric power consumption on a yacht (6) which used LPG (liquefied petroleum gas) for cooking and a diesel engine for auxiliary power. This study included generator and deep cycle lead acid battery performance tests and led to the specification of a 115 ampere-hour minimum daily charging capacity. The 200 W output machine represented a convenient prototype size with a generous 320 ampere-hour daily charging capacity.

To achieve a high power density, hydrogen would be used as the working fluid in a hermetically sealed and pressurized engine. Helium is next best to hydrogen in terms of good heat-transfer properties and low fluid friction, and is preferred because of its lower rates of loss through diffusion, safety and the absence of the risk of hydrogen embrittlement. The present engine needed to be rechargeable with working fluid in remote locations. This led to a decision to use air at a charge pressure of 1 MPa as working fluid, although its poorer heat-transfer and fluid frictional properties make it inferior to hydrogen or helium in regard to specific power output and efficiency (7, 8). The 1 MPa charge pressure can be achieved by a manual or battery-powered pump and was considered suitable from tests by Clucas and results of Walker (9), both on an air-charged Philips 102C engine.

With air as the working fluid, the risk of combustible mixtures in the hot gases must be avoided (10). This safety concern was addressed by using a dry crankcase and sealed-for-life single rotational degree of freedom rolling bearings only to minimize free combustible lubricants which could enter the hot-end working space. This feature is made possible by the design of the wobble yoke mechanism described earlier (2).

The heater combustion system is required to be quiet, clean, safe for stationary and mobile applications, use readily available fuel and provide a high-temperature heat source with low NO_x and other pollutant emissions. The 200 W prototype machine was designed to run with LPG fuel, but alternative fuels are currently being assessed, including renewables such as vegetable oils, alcohols and wood.

For a high specific power output, a high engine speed would be sought (>4000 r/min). To limit seal wear and flow friction losses using air as working fluid, speeds of less than 2000 r/min were desired. To reduce manufacturing costs an alternator design based on a conventional automotive unit was used. Its best efficiency occurred between 1400 and 1500 r/min. Using this speed range, the alternator shaft was made the main engine shaft, eliminating the need for gearing with its attendant cost, bulk and noise.

Power and efficiency increase with the temperature difference between the hot and cold ends, and the

hot-end temperature should be as high as possible. The hot-end material temperature was set at a maximum of 750 °C based on material operating limits. The cold-end temperature must be higher than the low-temperature sink (here ambient) and is important when looking for efficiency gains; for example a change of 10 °C at the cold end can have an equivalent effect on the ideal cycle efficiency ($\eta_{th} = 1 - T_k/T_H$) of a change of 30 °C at the hot end. For the combined heat and power objective, design calculations were based on a cold-end temperature of 50 °C. The cooling water temperature would be boosted using heat from the burner exhaust to a higher domestic hot water temperature if required.

In practice most high-performance kinematic engines with high power densities in the multi-kilowatt range use compact double-acting designs, although a single-cylinder beta or vee alpha configuration would meet the power requirements of the 200 W unit. Clucas (6) examined engine configurations at some length, including single-cycle alpha, two-cycle alpha, four-cylinder double-acting single-cycle beta and four-cycle beta forms (see Fig. 1). Equations offering closed-form solutions were developed or adapted for preliminary design for engine power output [see equation (1), a modification of the West equation (11)], heat transfer, cylinder wall and heat exchanger stresses, seal rubbing speed, overall engine volume, and shuttle loss and appendix losses [the last two using equations after Reader and Hooper (12)].

Predicted power and efficiency alone gave no clear winner from this design analysis, and a comprehensive decision matrix was constructed (6) to make a comparison which included a number of practical design and manufacturing criteria, engine complexity and the mass of costly materials. The four-cylinder double-acting arrangement was finally chosen on the basis of offering a large heat-transfer area for a given swept volume when using annular finned heat exchangers, a compact design, low vibration, smooth torque delivery and low starting torque. These advantages over other layouts appear to be enhanced as the design is scaled up.

Having decided engine mean cycle pressure and speed, swept volume was initially sized by using the empirical West equation:

$$BP = W_n P_{\text{mean}} f V_0 \frac{T_H - T_k}{T_H + T_k} \quad (1)$$

The West number, W_n , was selected by examining well-designed engines of similar power, speed and cycle pressure, giving $W_n = 0.25$. An inconsistency was noted in the literature on the value used for the engine total cycle volume variation, V_0 . Clucas (6) recommended that V_0 be taken as 1.414 times the expansion piston swept volume for alpha engines and equal to the power piston swept volume for beta and gamma types.

The engine was designed to be manufacturable in any competent machine shop (but suitable for high-volume production), able to be scaled up, self-regulating with minimal need for operator input, operated for a minimum of 5000 hours maintenance-free life before bearing or seal replacement, and air or water cooled. Important features of the engine are treated in more detail in Section 3.

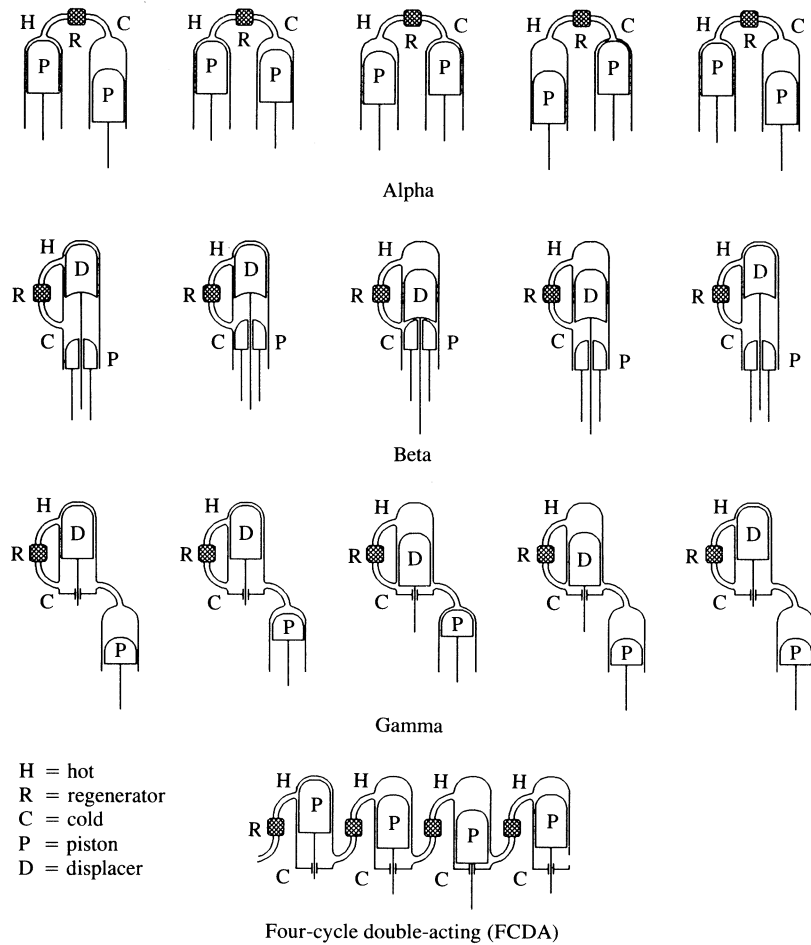


Fig. 1 Alpha, beta and gamma configurations. The four-cycle double-acting layout is a special case of the alpha configuration

3 OVERVIEW OF EMBODIMENT DESIGN

3.1 Engine layout

A cross-sectional view of the DMC 3 experimental single alpha configuration engine is shown in Fig. 2. The design principle used in this engine was carried across to the final DMC 5 pre-production prototype, which has a four-cylinder double-acting layout and is shown in Fig. 3. Both the DMC 3 experimental engine and the DMC 5 prototype used the wobble yoke mechanism (2) (patent pending) developed during the project. DMC 3 was a versatile engine specifically built for proof-of-principle testing, seal testing and experimental data acquisition for verification of the engine simulation. It was instrumented for measurement of expansion and compression space pressures, engine output torque and speed, and various temperatures. In one configuration it had an external electric motor coupled to the main shaft to carry out motoring tests and for driving the engine mechanism when the engine was built up as a piston seal test rig. Test results from this engine are given in Section 4. The following comments describe details of the later DMC 5 prototype illustrated in Fig. 3.

The alternator, whose rotor and stator are modelled closely on a commercial automotive brushless alternator design, is attached via a mounting flange to the cast LM25 aluminium alloy housing, which has external fins for cooling the alternator sealed within. The rotor

carrying the nutating bearing which creates the wobble motion is integral with the main shaft and also carries two balance weights which create a couple that almost completely balances the rotating out-of-balance couple generated by the motion of the pistons, as discussed by Clucas and Raine (2).

The nutating bearing may be manually adjusted in a slot in its rotor to vary the stroke of the engine. In future developments the stroke will be able to be varied from outside the engine as a means of instantaneous power control by dynamic swept volume variation, as previously demonstrated on the STM4-120 variable angle swash plate engine (10). Without the necessity for hydrodynamic lubrication when using the wobble yoke mechanism, engine starting may be achievable by rapid variation of the engine stroke (not yet attempted).

The alloy steel pistons run in filled PTFE (polytetrafluoroethylene, or Teflon) lip seals backed with O-rings and mounted in the housing. The very small angular movement of the piston rods is accommodated by an elastomeric joint between piston and piston rod. The piston caps are a thin stainless steel shell filled with an insulating material that minimizes parasitic heat loss from the hot end of the engine.

The cold-end heat exchanger assembly of stacked copper plates is clamped to the housing by bolting through the top cover plate into the main housing. The cooling water and gas flow passages are chemically machined as recesses in the plates, which are sealed

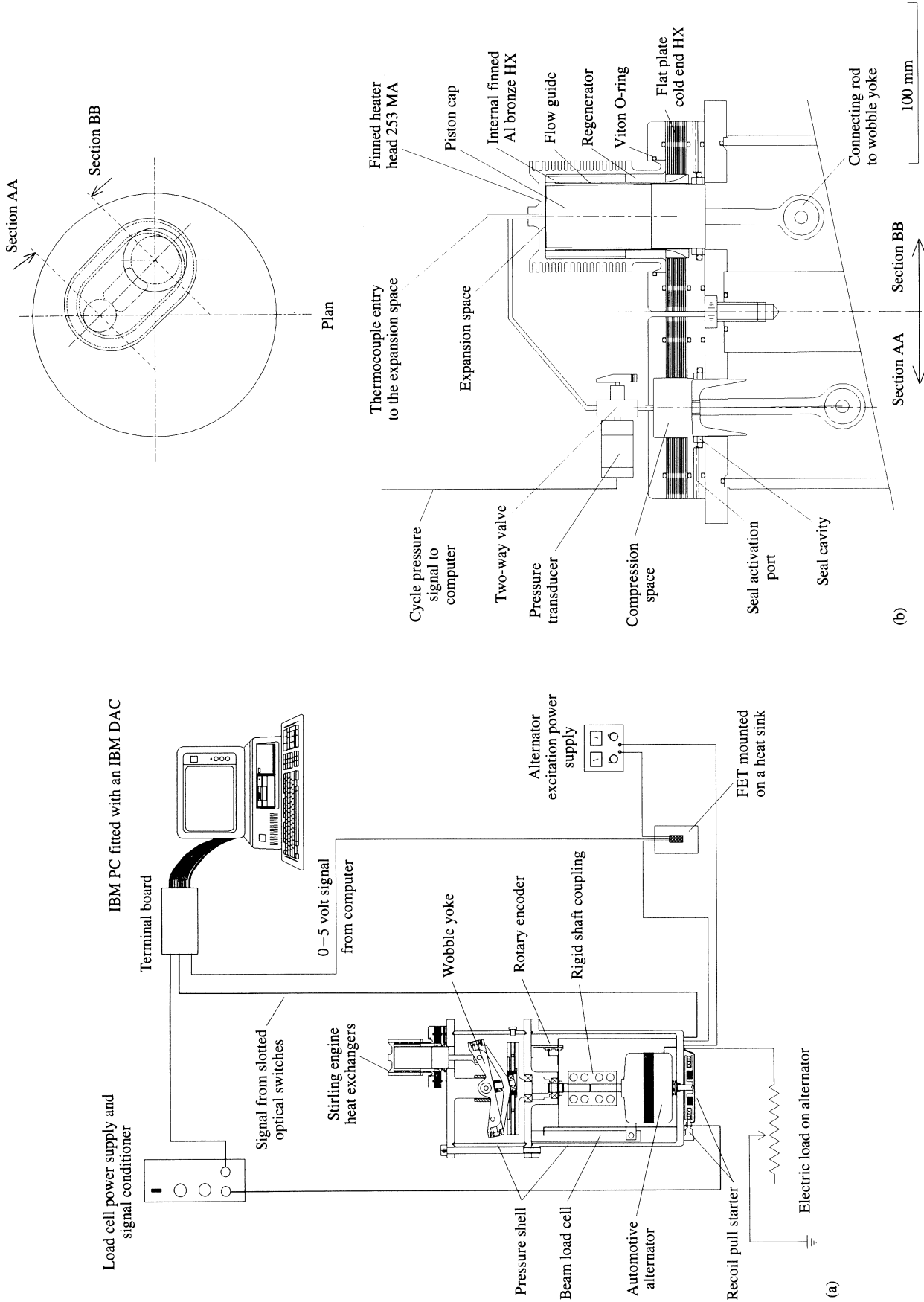


Fig. 2 (a) Hermetically sealed dynamometer for DMC 3 and the control equipment used (b) Cross-section of DMC 3 heat exchangers, pistons and seal cavities

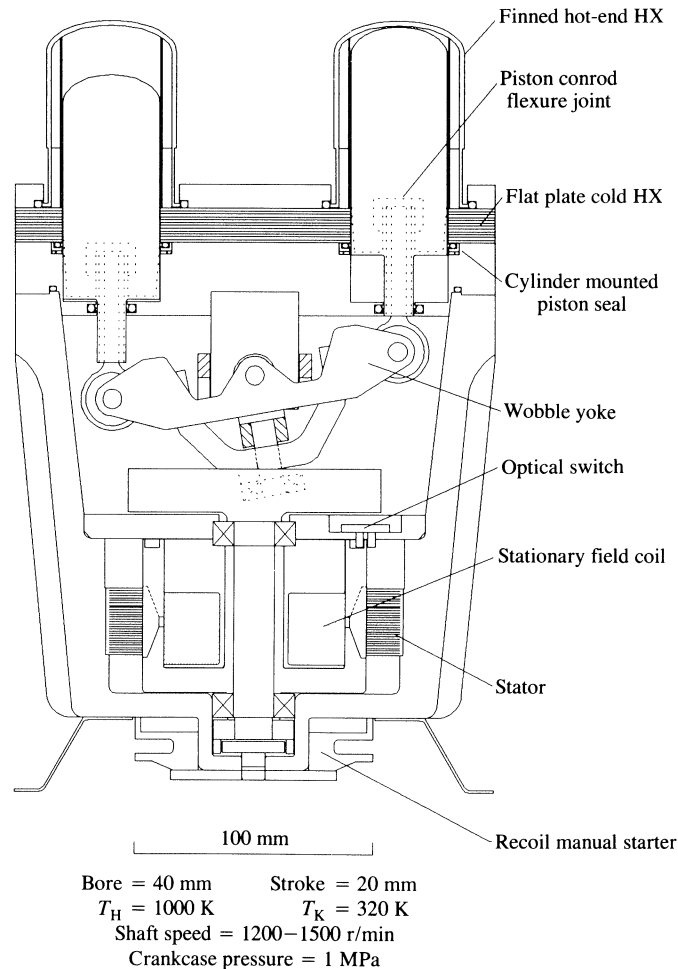


Fig. 3 DMC 5 prototype engine layout

together. This design was proven on DMC 3. The high-temperature stainless steel (Avesta 253MA) hot-end heat exchangers are externally finned and clamped in place on flanges at their base by means of the top cover plate of the engine housing, the joints incorporating O-ring seals for ease of assembly and reliability. The annular regenerator consists of stainless steel mesh wrapped on the internal regenerator sleeve.

The burner body is cast in a refractory ceramic material to give high radiant heat transfer and good insulation. A casting technique was developed which allowed all four plenum chambers surrounding the heater heads, the mixing tube, burner nozzles and combustion chambers to be cast in one operation (see Fig. 4). Current development is focused on a naturally aspirated pre-mixing burner of this style to achieve low noise and gas pressure requirement. A recuperator is to be developed to raise brake gross thermal efficiency from the present 12 per cent to a competitive level.

3.2 Alternator–starter motor

It is seen in Fig. 3 that the recoil starter, for manual starting, necessarily sits outside the hermetically sealed housing. A normally stationary shaft passes through an O-ring seal, which retains the 1 MPa system pressure and transmits the manual starting torque to the engine via a clutch. The engine is also designed to be electrically started. The stationary field alternator which does

not require slip rings doubles as an electric starter motor, simply achieved by switching the star-wound stator windings using three optical switches and three field effect transistors (FETs). The simplified circuit diagram is shown in Fig. 5.

Because of magnetic saturation of the stationary field coil, the prototype alternator developed gave a slightly

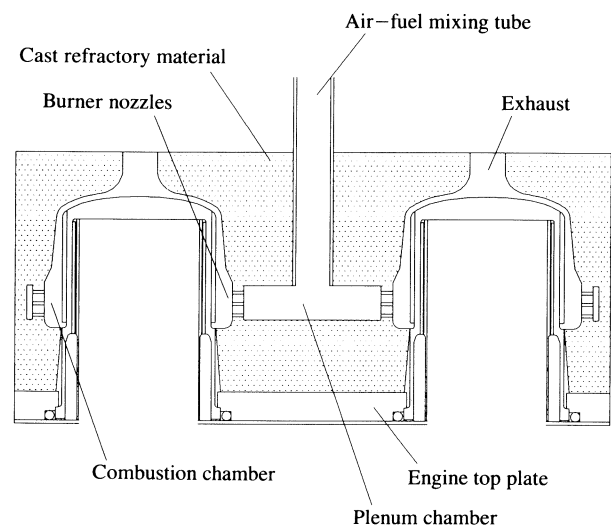


Fig. 4 Cross-section of the cast refractory burner/insulator for DMC 5

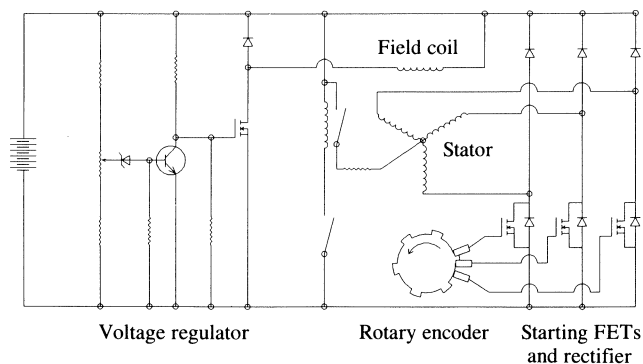
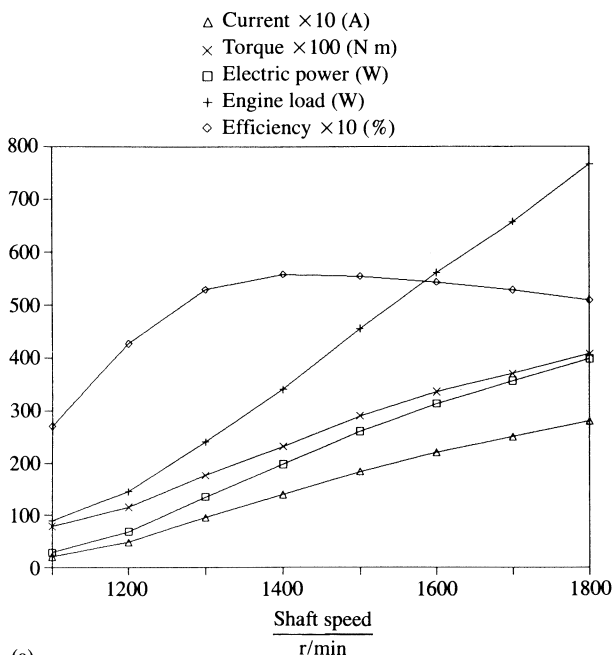
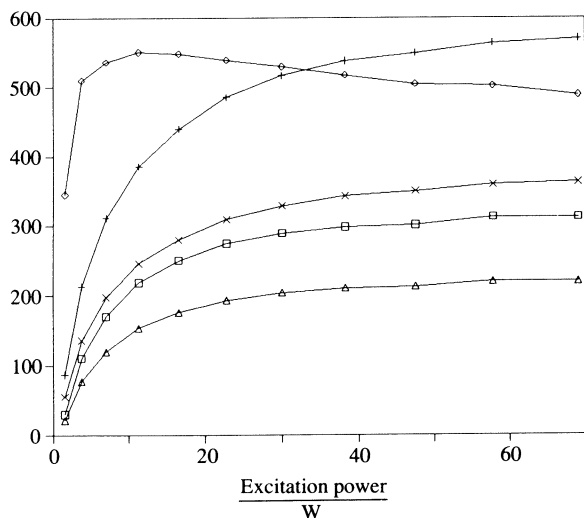


Fig. 5 Alternator-starter circuit diagram

lower performance than a comparable commercial slip ring automotive alternator, but easily met the power delivery requirements of 200 W at 1500 r/min for the battery charger system. Figure 6 shows the measured characteristics of the alternator on the DMC 5 engine, firstly with the excitation set to maintain the 14.2 V



(a)



(b)

Fig. 6 DMC 5 alternator characteristics

peak charging voltage and secondly with the speed held constant at 1500 r/min. Figure 6a shows that the optimum efficiency occurs between 1400 and 1500 r/min, 1500 r/min being the speed for which the engine heat exchangers were finally designed.

Figure 6b shows that the variation of power or load on the engine is very steep between 0 and 20 watts excitation power when driven at 1500 r/min. This feature enabled engine speed control by electronically varying the excitation power, a very convenient approach for a small system. Speed feedback was obtained by using a frequency-to-voltage converter on one phase of the three-phase alternator. On larger engines the approach taken to speed control will be by means of engine stroke variation. This change and the move to a higher voltage and larger alternator will allow higher generation efficiencies to be achieved over a wide range of engine power.

3.3 Seals

Many Stirling engines rely on the standard two splitting piston seals (10). For engines of fractional kilowattage power, the seal design is very critical, particularly when no fluid lubricant is present. Early tests with non-split single lip-type seals were made on a converted twin-cylinder two-stroke internal combustion engine, DMC 2 (6). This engine is an alpha configuration with piston-mounted carbon-filled Teflon lip seals. These experiments showed that the seals worked well the first time the engine was run, then refused to seal again until suitable pre-loading was applied. This is due to thermal expansion and creep of the seal material. In an attempt to utilize a single lip-type piston seal in a double-acting configuration engine, cylinder-mounted seals have been developed.

The DMC 3 test engine was fitted with cylinder-mounted lip seals with variable pre-loading by pressure-regulated nitrogen gas (Figs 2 and 7). With this system it is possible to tune the seal pre-loading to suit the engine operating conditions. Figure 8 shows the variation of indicated and brake power with various seal activation pressures (a different test series from that shown in Figs 10 and 11), and that there is an optimum seal activation pressure at which the indicated power reaches a plateau. Above this there is little or no seal leakage but shaft power decreases due to increased seal friction. This optimum seal pre-load was considered when designing the seals for the DMC 5 engine. Cylinder mounting of the seals reversed the earlier seal failure phenomenon. On start-up, the seal is shrunk on to the

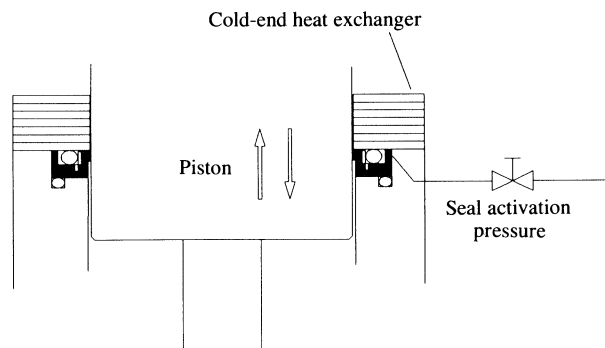


Fig. 7 Typical seal design used in DMC 3 test engine

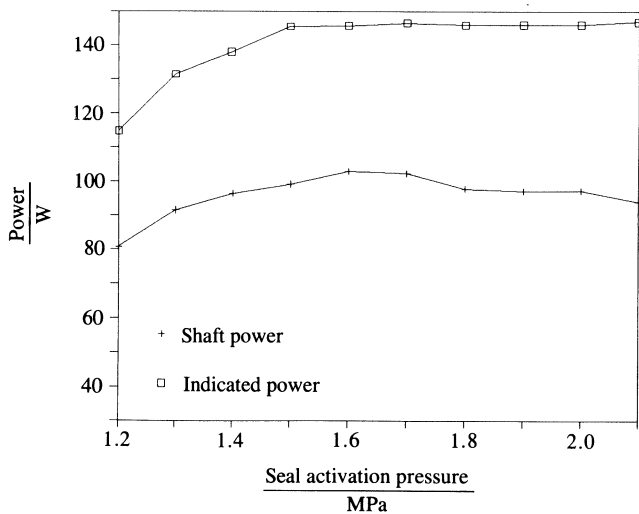


Fig. 8 Measured variation of indicated and shaft output power versus seal activation pressure for DMC 3 engine

piston, having cooled after the previous run, and a seal is created giving good starting conditions, but after running for several minutes the seal expands on heating and the seal leaks, stalling the engine. Application of the activation pressure restores the seal and the engine is then able to be started again. In the DMC 5 engine this activation pressure is provided by a circumferential metal spring backing the working part of the lip seal. Appropriate porting and O-ring backing provides gas pressure seal closing for the reversing pressure differential.

3.4 Heat exchangers

The form of the heat exchangers has already been outlined in Section 3.1. The design of the gas circuit for an efficient and compact Stirling engine is complex, as the working fluid is experiencing continuously changing velocity, density, temperature and pressure, making steady state heat exchanger design techniques unsuitable. Any temperature drop in the heat-transfer process decreases engine efficiency, so high wetted area and heat-transfer coefficients must be sought. This, however, can be detrimental to engine performance by increasing the cycle dead volume and flow resistance in the gas circuit. Lengthy computer programs for the gas circuit design are generally necessary.

The project programme dictated the adaptation of an existing simulation program code. Its requirements were to be:

- able to model the flow and heat-transfer processes adequately to enable the effect of changing component dimensions to be studied;
- available at reasonable cost as a listing to allow customization to match proposed design conditions;
- verifiable (DMC 3 was later used to verify trends predicted by the simulation).

Although more advanced thermodynamic design and engine scaling methods have more recently appeared (13–15), the listed quasi-steady flow model (QSFM) by Urieli and Berchowitz (1) met these requirements and was used in the design of DMC 3, and subsequently DMC 5. This model allows for the non-steady flow of

the gas during the working cycle by breaking the cycle into small increments over which steady flow conditions approximately prevail. The engine is divided up into a minimum of six cells: compression space, cooler, half-regenerator, half-regenerator, heater and expansion space. The energy equation for each cell can be generalized in the form:

$$\begin{aligned}
 & \text{(rate of heat transfer into the cell)} \\
 & + \text{(net rate of enthalpy convection into the cell)} \\
 = & \text{(rate of work done on the surroundings)} \\
 & + \text{(rate of increase of internal energy in the cell)}
 \end{aligned} \tag{2}$$

Based on equation (2) Urieli and Berchowitz (1) derived 40 equations, 13 of which are simultaneous differential equations. The effect of flow losses can be included in the simulation in a fashion that is not thermodynamically rigorous but enhances the agreement between the model and test bed results. This has been independently verified by I. Urieli (August 1994, Department of Mechanical Engineering, Ohio University, personal communication). A consistent set of initial conditions is determined from the designer's input data and the solution is obtained using the fourth-order Runge-Kutta method.

Additions or modifications to the published QSFM code (6) were:

- stability checking and modification of the time step if necessary to allow unattended processing of several thousand combinations of heat exchanger dimensions;
- heat-transfer conditions external to the heat exchangers;
- cycle volume variations according to the wobble yoke kinematics;
- calculation of the instantaneous fin efficiency of the annular finned heat exchangers;
- inclusion of flow entry, exit and bend pressure losses in the fluid circuit;
- routines for comparing the effects of various combinations of component dimensions.

The listed code did not allow easy interactive editing of the output data so a Stirling engine design aid (SEDA) spreadsheet program (6) was developed which allows the designer to develop an acceptable preliminary set of engine dimensions first, using simpler analyses such as equation (1), the Schmidt analysis and equations for appendix and shuttle losses. The SEDA then formats and writes an input file for the quasi-steady flow model which was used to check the chosen heat exchanger design or specified combinations of several variables. A sample set of the 27 variables passed to the QSFM for DMC 3 are given in Table 2. Output from the QSFM is retrieved by the SEDA spreadsheet program which is used to generate and edit the extensive tabular and graphical output (6).

Optimization of Stirling engine heat exchangers is complicated by the difficulty in defining an objective function. It is not sufficient just to optimize the power output or efficiency. For a commercially viable and manufacturable design there are objectives related to physical form, size and cost, and compromises must be

Table 2 Example of DMC 3 variables passed to the QSFM

Variable number and description	Value
1. Compression space clearance volume (10^{-6} m^3)	1.00
2. Compression space swept volume (10^{-6} m^3)	17.32
3. Expansion space clearance volume (10^{-6} m^3)	3.00
4. Expansion space swept volume (10^{-6} m^3)	25.13
5. Phase angle (deg)	90.00
6. Hot-end annular gap (mm)	0.35
7. Hot-end fin radial depth (mm)	3.50
8. Hot-end fin length (mm)	50.00
9. Hot-end gap number	100
10. Hot-end fin material conductivity (W/m K)	16.00
11. Hot-end external heat-transfer coefficient ($\text{W/m}^2 \text{ K}$)	20.00
12. Cold-end slot gap (mm)	0.35
13. Cold-end slot width (mm)	21.00
14. Cold-end slot length (mm)	60.00
15. Cold-end slot number	12
16. Cold-end fin external area (10^{-4} m^2)	983.00
17. Cold-end conductivity (W/m K)	360.00
18. Cold-end external heat-transfer coefficient ($\text{W/m}^2 \text{ K}$)	500.00
19. Internal regenerator diameter (mm)	42.00
20. External regenerator diameter (mm)	52.00
21. Regenerator length (mm)	25.00
22. Regenerator porosity	0.80
23. Regenerator wire diameter (mm)	0.04
24. Mean cycle pressure (MPa)	1.07
25. Hot-end temperature (K)	1023
26. Cold-end temperature (K)	323
27. Engine shaft rotational speed (r/min)	1500

made. It would be extremely complex to develop an algorithm to combine all these factors into an analytical objective function. It is also difficult to ensure that a numerical optimization routine will identify a global optimum. Several numerical packages for optimization of the heat exchangers were tried which required an objective function to maximize or minimize them. To reach a reliable best design, a comprehensive grid search technique was developed in which ranges of feasible (manufacturable) component dimensions were specified by the designer and all combinations of these dimensions were processed by the QSFM.

This procedure took minutes to program, but took 36 hours to run 1800 simulations on a 486 personal computer. From these simulations, a separate search algorithm selected several computed results that met the design requirements. Table 3 shows a sample set of

results for DMC 3, where the algorithm selected designs that predicted $\geq 163 \text{ W}$ brake power and ≥ 58 per cent indicated efficiency. From this reduced set of results the designer could select a most desirable design. The bottom two rows of Table 3 show the combinations that gave either maximum power or maximum indicated efficiency, each being able to be maximized at the expense of the other.

4 PERFORMANCE OF THE EXPERIMENTAL AND PROTOTYPE ENGINES

Experiments were run with the alpha configuration DMC 3 engine which represented one-quarter of the four-cylinder double-acting engine DMC 5. The DMC 3 engine was instrumented to measure pressures in the expansion and compression spaces during the engine cycle, and had a rotary encoder on the shaft. These features enabled P - V diagrams to be generated and indicated power to be calculated. Figure 9 shows simulated and measured P - V diagrams obtained from the QSFM and DMC 3 in over a hundred individual experiments on the engine prior to designing DMC 5. It is seen that further development of the modelling of fluid friction losses and adverse heat transfers at the expansion and compression spaces is required to improve the simulation of the cycle pressure range.

Measured and computer-simulated indicated power are plotted against speed in Fig. 10 for a range of engine strokes. A single scaling factor of 0.85 required to align model and test bed data has been included to facilitate the comparison and is seen to match experimental and computed results well across a wide performance range. The swept volume variation of DMC 3 was obtained by varying the nutating bearing offset. Varying other engine parameters gave similar trends (6), providing sufficient verification of the QSFM to allow its cautious use in the design process for DMC 5.

The circumferentially finned stainless steel heater head on DMC 3 initially had an internally finned aluminium bronze sleeve [similar to that on the Philips 102C engine (16)], press fitted into its bore, to act as the metal-to-working fluid heat exchanger. This was to give a high heat transfer with low dead volume. This finned

Table 3 Sample set of results for DMC 3 from the search algorithm

Design selection criteria	Simulation number	Brake power W	Indicated efficiency %	Hot-end fin gap mm	Hot-end HX length mm	Number of hot-end HX fins	Regenerator length mm	Cold-end HX gap mm	Regenerator outside diameter mm
Indicated power $\geq 163 \text{ W}$	607	163	58.5	0.20	30	80	25	0.3	50
	613	163	58.4	0.20	30	90	25	0.3	50
	619	164	58.3	0.20	30	100	25	0.3	50
	637	163	58.6	0.20	35	90	25	0.3	50
	643	163	58.4	0.20	35	100	25	0.3	50
Indicated efficiency $\geq 58\%$	745	163	58.1	0.25	35	70	25	0.3	50
	751	163	58.1	0.25	35	80	25	0.3	50
	775	163	58.2	0.25	40	80	25	0.3	50
	781	163	58.2	0.25	40	90	25	0.3	50
	787	163	58.0	0.25	40	100	25	0.3	50
Maximum indicated power	19	173	56.1	0.2	30	100	20	0.3	50
Maximum indicated efficiency	1299	131	63.3	0.2	50	70	30	0.3	54

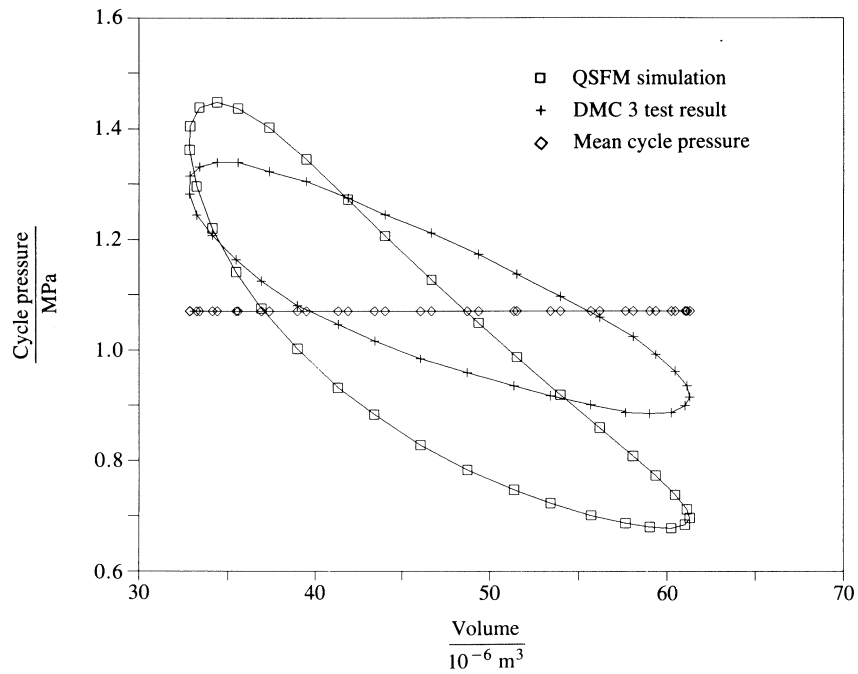


Fig. 9 Comparison between simulated and measured indicated power for DMC 3 (data as for Table 2)

component was expensive and the simulation indicated that the required design performance could be attained by replacing the finned sleeve with a plain sleeve giving an annular gap. A sample of simulated and experimental shaft brake power results for DMC 3 are shown in Fig. 11a and b respectively. It is seen that operation with the much less costly plain internal sleeve, and a 0.6 mm annular gap to the inner wall of the stainless steel heater head, produced power output close to that with the aluminium bronze finned sleeve fitted in both the simulation and the test bed engine. Figure 11 shows that there is good agreement between the trends of the computer model and experimental results for annular

gaps of 0.4 mm or more, but the present QSFM simulation does not model the suboptimal smaller gaps well where fluid friction is very high and test bed power deteriorates rapidly.

The best steady state power at design conditions from the single-cycle DMC 3 experimental engine was 109 W, and it was possible to move with confidence to the four-cycle double-acting arrangement which required production of at least 360 watts to ensure an alternator output of 200 W. The results of computer modelling and DMC 3 prototype testing led to the choice of 40 mm bore, 20 mm stroke, 14 mm rigid piston rod sleeve diameter and 60 mm cylinder pitch circle radius for the

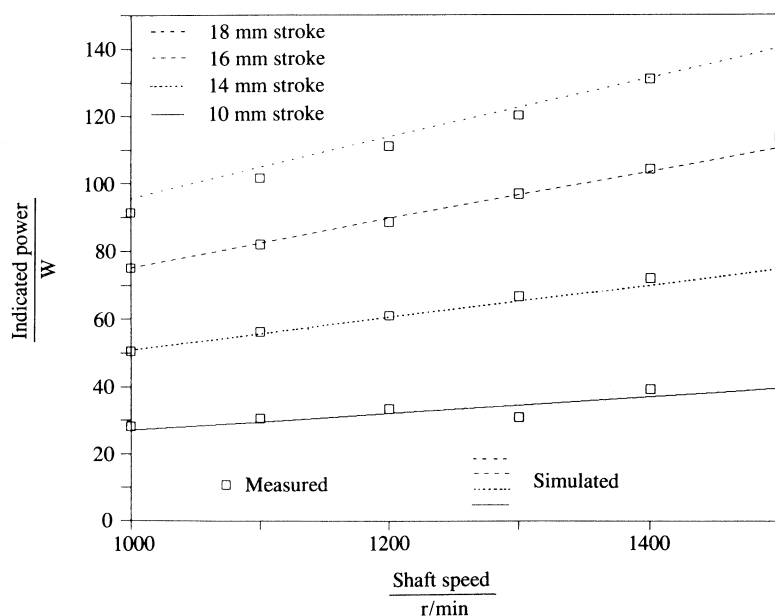
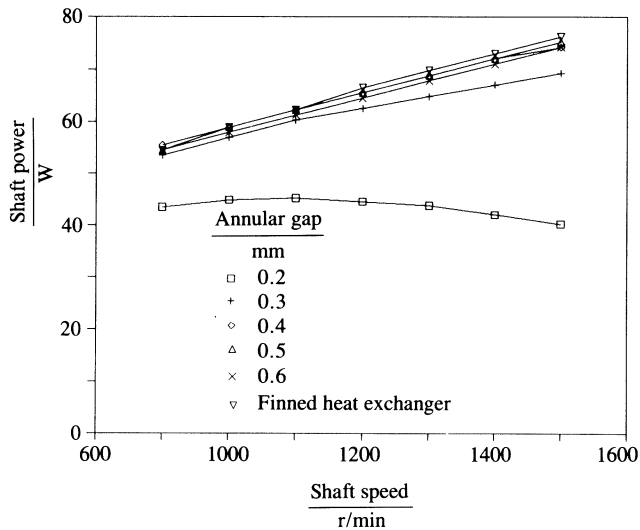
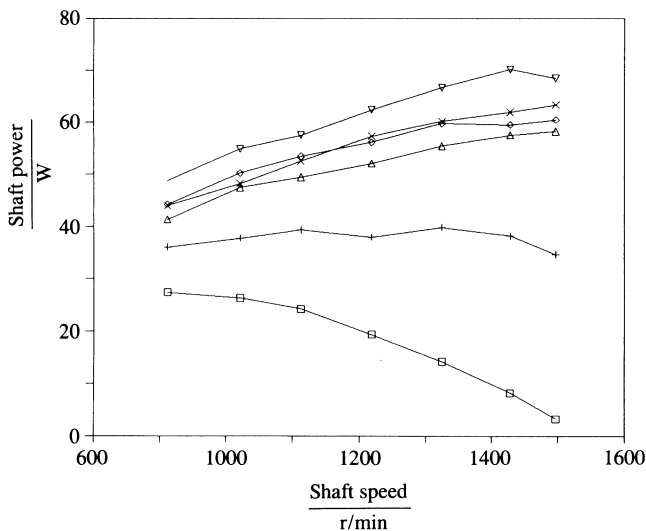


Fig. 10 Comparison of measured and simulated power for DMC 3 engine with varying stroke



(a) Simulated brake power



(b) Measured brake power

Fig. 11 DMC 3 shaft power for various values of hot-end annular gap compared with the finned insert

DMC 5 prototype. DMC 5 stainless steel heater heads to date have had longitudinal external fins and a smooth internal bore creating an annular gap giving a compromise between low cost and ultimate performance. The design brake power of 400 W (mechanical) has been exceeded in recent tests using this simpler system. This engine has now run for about 120 hours and at its design speed of 1500 r/min has comfortably exceeded the design output power of 200 W electrical power in continuous running. Full temperature and pressure instrumentation of the DMC 5 engine has yet to take place, but gross thermal efficiency is approximately 12 per cent prior to inclusion of a recuperative burner.

Preliminary motoring tests have also explored the heat pumping potential of DMC 5. Motored in its normal prime mover direction of rotation, the hot-end

heater heads fell to -110°C in 10 minutes. Motored in the opposite direction the hot-end heater heads rose from ambient temperature to 320°C in 10 minutes. Further research into refrigeration equipment based on this engine design is intended.

5 CONCLUSION

This paper has described the design development and embodiment of a hermetically sealed four-cylinder double-acting Stirling engine driving an integral alternator providing 200 W 12 V d.c. electrical output for charging batteries. Performance modelling using the SEDA and QSFM simulations to advise suitable engine dimensions and experimental work with a single-cycle alpha experimental engine gave a reliable benchmark on which to base the dimensions of the later four-cylinder double-acting engine. While the design was aimed at the yachting, mobile home and small remote dwelling market, strong interest in a larger 3 kW version from an electric power supply authority means that the 3 kW unit will be prototype tested with stroke control for power variation while burner development and endurance testing of the 200 W unit proceeds.

REFERENCES

- Urieli, I. and Berchowitz, D. M. *Stirling cycle engine analysis*, 1984 (Adam Hilger Ltd, Bristol).
- Clucas, D. M. and Raine, J. K. A new wobble drive with particular application in a Stirling engine. *Proc. Instn Mech. Engrs, Part C*, 1994, **208**(C5), 337–346.
- Calder, N. *Boatowner's mechanical and electrical manual*, 1990 (Nautical Books, A & C Black Ltd, London).
- Bartolini, C. M., Pelagalli, L. and Vincenzi, G. Experimental analysis and test results of small Stirling engine prototype. Proceedings of Fifth International Stirling Engine Conference, Dubrovnik, 1991, Appendix, p. 9.
- Walker, G., Scott, M. J. and Bingham, E. R. Ross–Stirling silent boat engine. Proceedings of Fifth International Stirling Engine Conference, Dubrovnik, 1991, p. 327.
- Clucas, D. M. Development of a Stirling engine battery charger based on a low cost wobble mechanism. PhD thesis, Department of Mechanical Engineering, University of Canterbury, New Zealand, 1993.
- Walker, G., Reader, G. T., Fauvel, O. R. and Bingham, E. R. The Stirling alternative. Department of Mechanical Engineering, The University of Calgary, 1994.
- Li, X. Design of the low power Stirling engine—possible application to irrigation in rural areas of China. PhD thesis, University of Reading, 1988.
- Walker, G. *Stirling engines*, 1980 (Clarendon Press, Oxford).
- Hargreaves, C. M. *The Philips Stirling engine*, 1991 (Elsevier, New York).
- West, C. D. *Principles and applications of Stirling engines*, 1986 (Van Nostrand Reinhold Co., New York).
- Reader, G. T. and Hooper, C. *Stirling engines*, 1983 (E. & F. N. Spon, London).
- Organ, A. J. *Thermodynamics and gas dynamics of the Stirling cycle machine*, 1992 (Cambridge University Press).
- Organ, A. J. 'Natural' coordinates for analysis of the practical Stirling cycle. *Proc. Instn Mech. Engrs, Part C*, 1992, **206**(C6), 407–416.
- Organ, A. J. Anatomy of the Stirling cycle. *Proc. Instn Mech. Engrs, Part C*, 1993, **207**(C3), 161–173.
- de Brey, H., Rinia, H. and van Weenen, F. L. Fundamentals for the development of the Philips air engine. *Philips Tech. Rev.*, 1947, **9**.